

# Bridging Electrical and Structural Interface Properties: a Combined DFT-GW Approach

L. R. C. Fonseca<sup>1</sup>, P.Y. Prodhomme<sup>2</sup>, and P. Blaise<sup>3</sup>

<sup>1</sup> Wernher von Braun Center for Advanced Research, Av. Perimetral Norte 301, Campinas, SP 13098-381, Brazil, e-mail: fonseca@vonbraunlabs.com.br

<sup>2</sup> Freescale Semiconductor c/o CEA/Leti-Minatec, 17 Rue des Martyrs, 38054 Grenoble Cedex 9, France

<sup>3</sup> CEA/Leti-Minatec, 17 Rue des Martyrs, 38054 Grenoble Cedex 9, France

## ABSTRACT

The selection of a proper metal for replacement of polycrystalline silicon as the metal gate in future generation transistors has been hampered by pinning of the metal Fermi level at the metal/dielectric interface. Using monoclinic hafnia and zirconia as the gate dielectric we compare three different metal gate/gate dielectric interface structures where the oxygen affinity of the metal gate varies from low to high under normal processing conditions. For each of the metal gate/gate dielectric combination we considered a number of interface stoichiometries and tried to identify the most likely interface composition by comparing the calculated and measured valence band offsets (VBO). Because density functional theory (DFT) underestimates the dielectric band gap, it also underestimates the VBO thus requiring a correction to the band edges, which we accomplished using GW for cubic and monoclinic hafnia. Our GW shift value for monoclinic hafnia (0.3 eV) indicates mostly reduced interfaces in all metal/dielectric combinations considered.

**Index Terms:** high- $\kappa$  dielectrics, interfaces, band alignment, density functional theory, GW.

## 1. INTRODUCTION

To continue the historical trend of transistor performance enhancement the necessary miniaturization of device dimensions involves, among other things, thinner gate oxides, reduced channel length, and reduced junction depth [1]. In particular, the thinning of the SiO<sub>2</sub> layer has resulted in considerable power loss through leakage current in the dielectric, a problem that will become severe as the current scaling trend continues. To allow for further reduction of the equivalent gate oxide thickness (EOT) the replacement of SiO<sub>2</sub> by a high- $\kappa$  material such as ZrO<sub>2</sub> or HfO<sub>2</sub> (or corresponding silicates and nitrides), La<sub>2</sub>O<sub>3</sub> (or corresponding aluminates), or more complex oxide alloys must be considered [2]. The depletion length in the current polycrystalline silicon (poly-Si) gate technology also imposes a lower boundary on EOT, incompatible with future generations of complementary metal-oxide-semiconductor (CMOS) technology [1]. Moreover, it was recognized that new high- $\kappa$  materials can react with the polySi gate causing undesirable electrical property changes, like Fermi level pinning at the interface which results in large threshold voltages [3]. All these problems may be

overcome by the adoption of a high- $\kappa$  gate dielectric to replace SiO<sub>2</sub> and suitable metal gates to replace polySi.

The use of metal gates in a PMOS (NMOS) transistor requires a close alignment of the metal Fermi level with the silicon valence (conduction) band edge in the substrate. For bulk MOSFET devices the optimal metal work functions (WFs) should be within  $\pm 0.1$  eV of both the Si valence band edge for PMOS and the conduction band edge for NMOS [4]. While it is relatively easy to control the Fermi level of polySi through appropriate doping, the Fermi levels of metals are not so readily manipulated. This requirement imposes severe constraints on the identification of metal gates with suitable WFs and forming stable interfaces with the oxide under typical processing conditions. In addition to that, it is well-known that a metal WF on an oxide can differ significantly from its vacuum WF due to the formation of interface dipoles, which are usually attributed to the presence of interface states in the band gap of the oxide [5]. The origin of these states has been subject of intense debate in recent years. Some of the leading models describe them as surface states [6], metal-induced gap states (MIGS) [7-9], or disorder-induced gap states (DIGS)

[10]. These theories predict different distributions of states in the band gap, and some propose that those distributions depend only on the nature of the oxide and not on the details of the interface which makes them of great practical interest [5].

However, there are past experimental results [11,12] which cannot be explained with the ideas of gap states and by models that only depend on bulk properties of the dielectric. In particular recent experiments of Mo gate electrodes on hafnia indicate a much weaker Fermi pinning than predicted by most models [4]. The measured Mo effective work function ( $W_{\text{Feff}}$  – a measure of the alignment between the band edges of the Si substrate and the metal Fermi level, or similarly the flat band voltage [13]) on hafnia was 4.95 eV and on SiO<sub>2</sub> 5.05 eV, while the maximum Mo vacuum WF is 4.95 eV [14]. The close agreement between  $W_{\text{Feff}}$  and vacuum WF characterizes weak Fermi pinning. A similar behavior has also been observed for composite metals such as TiN [15] and HfN [16], where the metal  $W_{\text{Feff}}$  on HfO<sub>2</sub> was actually slightly larger than on SiO<sub>2</sub>. These deviations from predictions of theories based on the bulk properties of the dielectrics can be explained by the formation of new metal-oxide specific interface states, which possess a net dipole moment. One possibility is the formation of Mo-O bonds at the interface, which are polarized and can lead to an increase of the metal  $W_{\text{Feff}}$  on hafnia. Such interface configuration is meaningful due to the proneness of Mo surfaces to oxide.

On the other hand in Ref. [17] it was found that the platinum  $W_{\text{Feff}}$  on HfO<sub>2</sub> is very low and varies, ranging between 4.6 and 4.9 eV (the Pt vacuum WF is ~5.6 eV), depending on the oxygen partial pressure during forming gas anneal (FGA). The same band offset instability under oxygen annealing was reported for other late transition metals [18]. Interface reaction is not responsible for such large work function shift as it has been experimentally shown [19] that the Pt/HfO<sub>2</sub> interface is stable for annealing at 5000C for 1 hour: experimental data show a sharp interface with very low interface diffusion between Pt and HfO<sub>2</sub> at this temperature.

Another technologically relevant and well studied system is the WC/HfO<sub>2</sub> stack. A number of experimental works have explored the growth of WC films using different deposition techniques [20-26]. In Ref. [20] tungsten-carbon layers with a stoichiometric composition of W : C = 1 : 1 were deposited on Si forming a single polycrystalline phase by DC magnetron sputtering. It was shown that both W- and C- terminated surfaces (denoted by WC-W and WC-C, respectively) can be obtained during deposition. Theoretical studies of WC surfaces were performed in Refs. [27,28]. It was found that W- termination has

the lowest surface energy and a vacuum WF of 5.2-5.3 eV, which meets the requirements for PMOS transistor devices. However, it is shown in Ref. [29] that interaction of oxygen with the WC(0001) surface leads to removal of carbon atoms from the (sub)surface layers. Similar modifications can proceed at a WC/oxide interface.

In this paper we aim to correlate the oxygen affinity of Pt, Mo, and WC with their  $W_{\text{Feff}}$  values on hafnia and zirconia. The interface approximate chemical composition is obtained by fitting to experimental data on the metal  $W_{\text{Feff}}$  through the variation of the concentration of oxygen in the model interface. From these results a more general correlation between the metal species and its  $W_{\text{Feff}}$  may be possible. However, the chosen theoretical method for evaluating the metal/dielectric band alignment is limited in its capacity to predict correct band gaps and valence band offsets, thus a direct and quantitative comparison with experiment is not possible [30]. For this end we calculate and employ a GW-derived shift to our approximate band offsets. We present a discussion on GW and argue that the level of approximation adopted here should be a first step towards an accurate model for band offset calculations. The consequences to the band offset and interface stoichiometry are discussed.

## 2. COMPUTATIONAL DETAILS AND INTERFACE MODELS

The properties of the Pt surface and of the interface between Pt and monoclinic hafnia (Pt/m-HfO<sub>2</sub>) were investigated using density functional theory (DFT) [31], with core electrons replaced by pseudopotentials (PPs), and valence states described by a plane wave (PW) basis set as implemented in the VASP code [32]. Both local density approximation (LDA) [33] and generalized gradient approximation (GGA) in the PW91 form [34] were used for comparison. Ultrasoft non-local PPs [35] were used for all the atomic species. Relativistic PPs for Hf and Pt were obtained using the neutral atomic configurations 5d36s1 and 5d96s1, respectively. The PW basis was expanded up to a cutoff energy of 600 eV for bulk calculations and 396 eV for interface calculations; sampling of k-space was done using a 5x5x1 k-point Monkhorst-Pack grid for interface calculations based on the (1x1) m-HfO<sub>2</sub> unit cell vectors in the interface plane. The structures of all slabs were fully optimized until the maximum residual force was less than 0.07 eV/Å. The calculated bulk lattice constant of fcc Pt ( $a = 2.763 \text{ \AA}$ ) is in good agreement with its experimental value  $a = 2.775 \text{ \AA}$  [36]. The calculated cell vectors of the m-HfO<sub>2</sub> phase ( $a = 5.015 \text{ \AA}$ ,  $b = 5.123 \text{ \AA}$ ,  $c = 5.161 \text{ \AA}$ , and  $\beta = 99.51^\circ$ ) are within typical

LDA/DFT error from experimental data ( $a = 5.117 \text{ \AA}$ ,  $b = 5.175 \text{ \AA}$ ,  $c = 5.295 \text{ \AA}$ , and  $\beta = 99.18^\circ$  [37]). The calculated oxygen adsorption energy on different sites of the Pt(111) surface using a model slab containing 9 Pt layers (not shown) are also in reasonable agreement with previous theoretical results [38-40].

The structural and electrical properties of bulk Mo and monoclinic zirconia (m-ZrO<sub>2</sub>), and of Mo/m-ZrO<sub>2</sub> interfaces were also investigated using DFT/LDA/PP, but in this case the valence states were described by a basis set comprised of linear combinations of numerical atomic orbitals (LCAO) as implemented in the SIESTA code [41]. The single zeta plus polarization (SZP) basis set was used for the LCAO. Norm-conserving non-local PPs [42] of the Troullier and Martins type [43] were used for all the atomic species. Relativistic PPs for Zr and Mo were generated for the neutral atomic configurations 4p64d25s2 and 4p64d55s1, respectively, which included the 4p electrons as valence states. To check the accuracy of our approach, we compared LCAO and plane-wave (PW) results. For the latter, ultrasoft PPs [44] as implemented in VASP were used. The bulk lattice constant for bcc Mo calculated using the LCAO basis is 3.15 Å, in excellent agreement with the experimental value of 3.147 Å [45]. The calculated cell vectors of the m-ZrO<sub>2</sub> phase ( $a = 5.04$ ,  $b = 5.24$ ,  $c = 5.10 \text{ \AA}$  and  $\beta = 97.63^\circ$ ) are within typical LDA/DFT error from experimental data ( $a = 5.15$ ,  $b = 5.21$ ,  $c = 5.31 \text{ \AA}$  and  $\beta = 99.23^\circ$  [46]).

The bulk and surface structural and electrical properties of WC and of WC/m-HfO<sub>2</sub> interfaces were investigated using LDA and GGA, within PP/PW as implemented in VASP. Relativistic PPs for W were generated for the neutral atomic configuration 5d56s1. The PW basis was expanded up to a cut-off energy of 497 eV and sampling of k-space was done using an 11x11x11 k-point Monkhorst-Pack grid for the WC hexagonal bulk phase and a 5x5x1 grid for interface calculations. The structures of all slabs were fully optimized until the maximum residual force was less than 0.07 eV/Å. Our calculated bulk lattice constants for hexagonal WC are  $a = 2.880 \text{ \AA}$  and  $c = 2.802 \text{ \AA}$ , in good agreement with the experimental values of 2.91 and 2.84 Å, respectively [45]. The calculated WC formation energy with respect to W(bcc) and C(diamond) is -0.48 eV, which is also in good agreement with the experimental value of -0.42 eV [47].

In order to investigate Pt(111)/m-HfO<sub>2</sub>(001) interfaces we considered five possible oxygen contents at the interface, ranging from a full oxygen monolayer (1 ML, 4 O atoms/small cell) to an oxygen-free interface (no oxygen atoms between the Pt and HfO<sub>2</sub> slabs) (see Figure 1) in steps of 0.25 oxygen MLs. To find the most stable interface structure for given oxy-

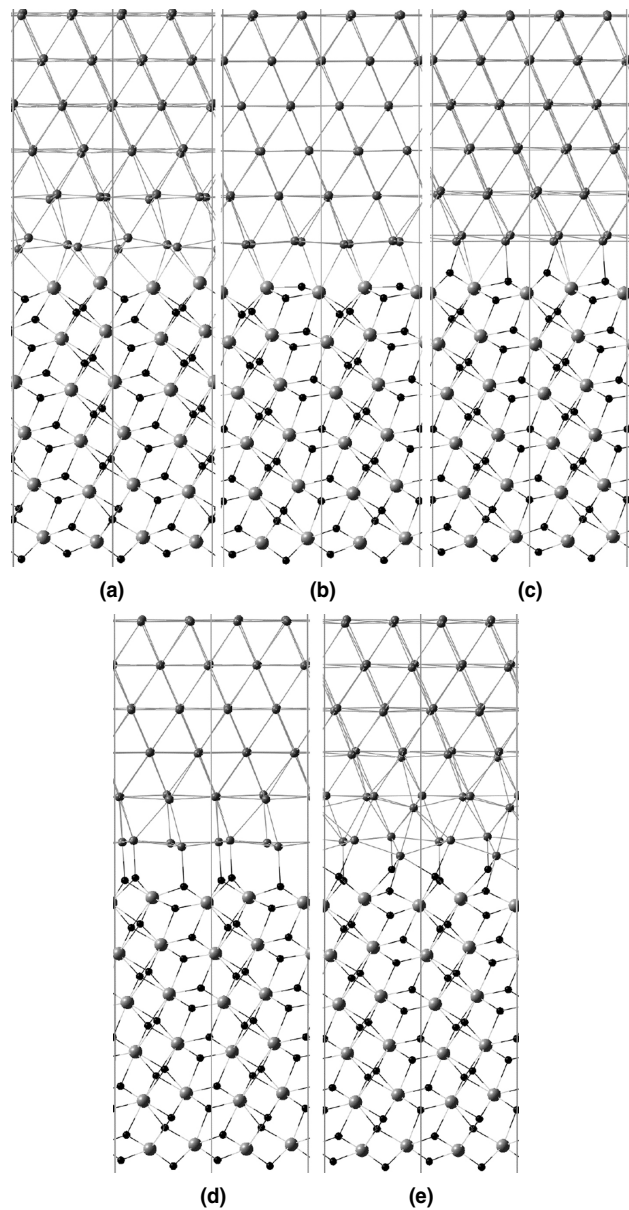


**Figure 1.** Fully relaxed Pt/HfO<sub>2</sub> interface models containing different oxygen concentrations: (a) 0 ML, (b) 0.25 ML, (c) 0.5 ML, (d) 0.75 ML, (e) 1 ML. Black : O, large gray: Hf, small gray: Pt (from Ref. 48).

gen content at the interface we applied the following approach. First, we constructed a slab consisting of three Pt and two hafnia MLs and the corresponding number of oxygen atoms between them. The initial relative lateral alignments of the Pt and hafnia slabs were chosen randomly. Those systems were then subjected to simulated annealing (molecular dynamics (MD) for 5000 2-fs steps and temperature quenching from  $T = 1000\text{K}$  to  $500\text{K}$ ). Next we selected the geometry with the lowest potential energy from the MD runs, extended the oxide thickness, and optimized the resulting structure. Last, we extended platinum slab thickness and once again optimized the new

structure. The resulting systems (one for each interfacial oxygen concentration) contain 6 Pt(111) MLs (with a thickness of 11 Å) and 6 m-HfO<sub>2</sub>(001) MLs (with a thickness of ~15 Å), and a vacuum gap ~15 Å thick.

The stoichiometric Mo(110)/m-ZrO<sub>2</sub>(001) interface was constructed using a  $\{(2,0),(-1,2)\}$  super cell, which results in about 7% Mo surface area mismatch with respect to the zirconia cell. The Mo super cell was fitted to zirconia which seems a reasonable choice since in typical experimental conditions the metal is deposited on the dielectric surface, thus the first metal MLs should adjust to the underlying dielectric atomic structure. The interface stress is likely to be relieved by interface defects (not considered in our models) or by bulk defects in Mo after the deposition of several Mo MLs. Slabs containing 6 Mo and 6 O-terminated m-ZrO<sub>2</sub> layers (not including the interfacial MoO<sub>x</sub> layer) were constructed and joined at one interface, with the other two surfaces separated by a vacuum gap 10 Å long. Figure 2 shows the four Mo/m-ZrO<sub>2</sub> model interfaces created for this study: (a) stoichiometric; (b) O-rich interface with two additional O atoms; (c) Mo/MoO<sub>x</sub>/m-ZrO<sub>2</sub> interface with subsurface oxidation of Mo; and (d) a reduced Mo/m-ZrO<sub>2</sub> interface (with less 0.5 ML of O atoms with respect to the stoichiometric case).

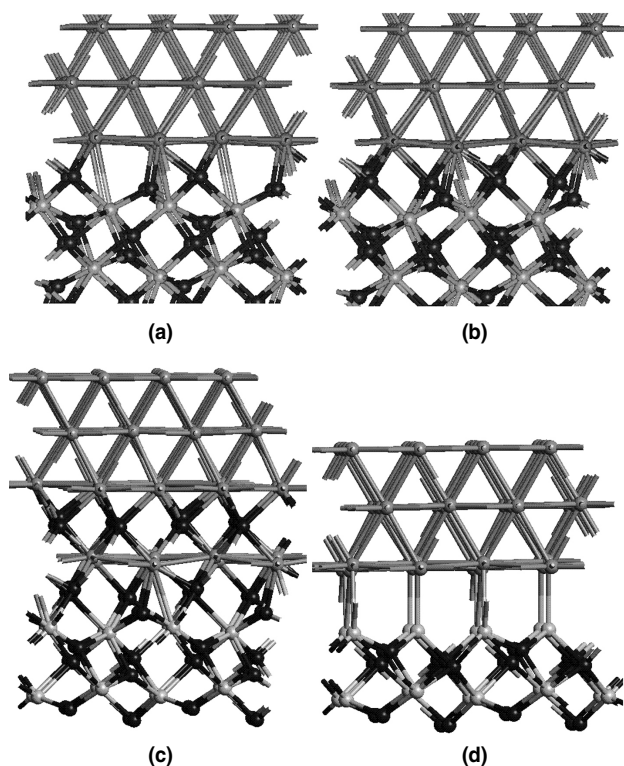


**Figure 2.** Structure of the Mo(110)/m-ZrO<sub>2</sub>(001) interfaces: (a) stoichiometric, (b) 0.5 ML O-rich interface, (c) 1.5 ML O-rich interface with subsurface Mo oxidation, (d) O-poor interface. Light gray: Zr; black: O; gray: Mo (from Ref. 49).

Models for the WC(0001)/m-HfO<sub>2</sub>(001) interface were constructed using a  $(2x\sqrt{3})$  super cell on the WC(0001) surface. Since the lattice parameters for m-HfO<sub>2</sub> ( $a = 5.117$  Å,  $b = 5.1754$  Å) and WC ( $a = 5.033$  Å,  $b = 5.812$  Å for the  $(2x\sqrt{3})$  cell) are significantly different, the WC structure was expanded along a by 1.7% and contracted along b by 11%. Despite the considerable artificial deformation introduced by our lattice matching procedure, test calculations for the contracted structure of WC demonstrated that its calculated WF is rather insensitive to this deformation (the WF of the contracted slab is only 0.2 eV smaller than that of the non-contracted slab). In order to model possible interfaces, we used slabs containing HfO<sub>2</sub> and WC layers without any vacuum gap. The slabs contain 6 W layers of WC and 6 layers of HfO<sub>2</sub> and involve two identical HfO<sub>2</sub>/WC interfaces. Figure 3 shows the five WC(0001)/m-HfO<sub>2</sub> model interfaces created for this study: (a) full monolayer (ML) of oxygen at the interface; (b) full ML of C at the interface; (c) half ML of O at the interface; (d) half ML of C at the interface; (e) only direct W-Hf bonds at the interface.

## A. Pt/HfO<sub>2</sub> Interface Structures and Properties

The most stable structures of Pt/HfO<sub>2</sub> found with simulated annealing for different oxygen content (0, 0.25, 0.5, 0.75, and 1 ML) at the interface are shown in Figure 1. The oxygen-free interface (0 ML-O) has only Pt-Hf bonds (7 bonds within the super cell with lengths in the range 2.65-2.81 Å). Insertion of one oxygen at the interface per two Hf atoms (0.25 ML-O) does not lead to the formation of Pt-O bonds, but reduces the number of Pt-Hf bonds from 7 to 5 and increases their average length (lengths in the range 2.66-2.99 Å). Only for the stoichiometric interface (two O atoms per two Hf atoms, or 0.5 ML-O) Pt-O bonds are formed (two bonds within the super cell with lengths 2.185Å and 2.065Å), while three Pt-Hf bonds still remain and are further stretched (2.995-3.115 Å). Pt-Hf bonds completely disappear at 0.75 ML-O at the interface (3 O atoms per two Hf atoms), and the number of Pt-O bonds increases to 3 with lengths 1.996Å, 2.055Å, and 2.132Å. These three interfaces are nearly flat. Increasing the oxygen content to 1 ML-O results in significant roughening of the interface, which is caused by repulsion between the oxygen ions at the interface. In this case the number of Pt-O bonds increases to 6 with two oxygen atoms forming a single Pt-O bond with lengths 2.027Å and 2.103Å, and two oxygen atoms forming a pair of Pt-O bonds with lengths (2.117 Å, 2.169 Å) and (2.003 Å, 2.048 Å).

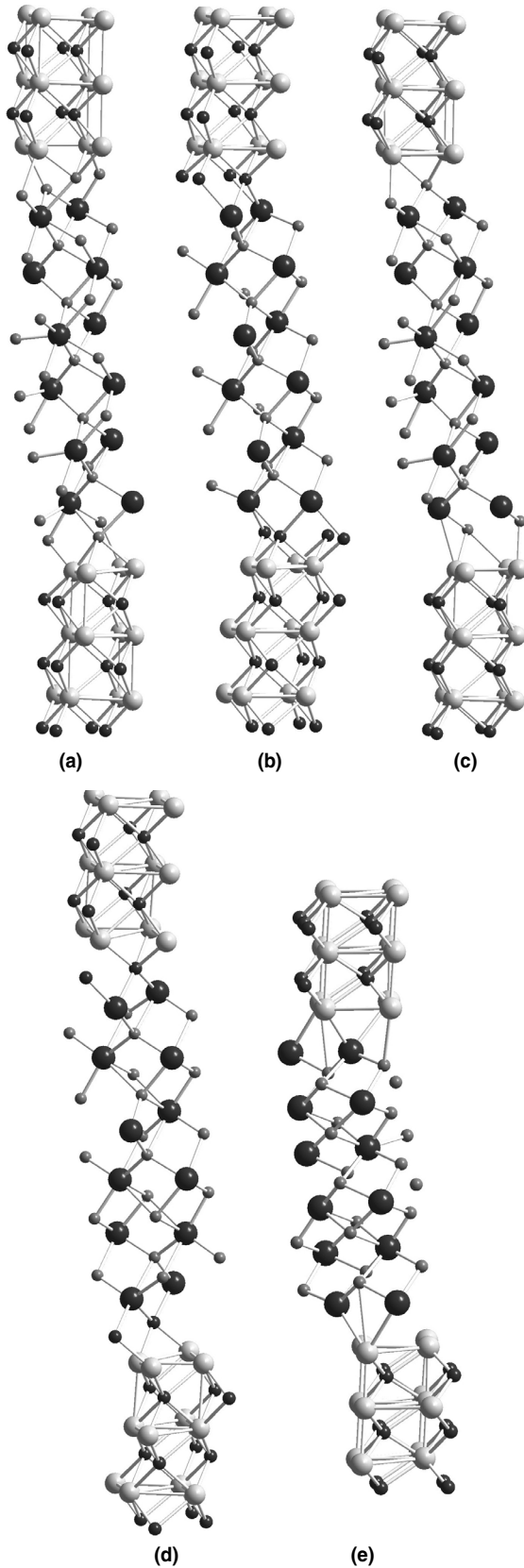


**Figure 3.** Optimized structures of WC/HfO<sub>2</sub> interfaces with various interfacial layers between Hf and W: (a) one ML O, (b) one ML C, (c) half ML O, (d) half ML C, and (e) no intermediate layer. Large light gray: W; large dark gray: Hf; small medium gray: O; small dark gray: C (from Ref. 50).

For each interface in Figure 1 we calculated the valence band offset (VBO - see Table I) using projected density of states (PDOS) analysis. The PDOS results were verified with the planar averaged potential (PAP) method of Van de Walle and Martin [51], in which the electrostatic potential across the slab is calculated in conjunction with an additional bulk calculation for each material to obtain the VBO.

It is seen from Table I that the calculated VBO drops sharply with the increase of the oxygen concentration, from ~3.0 eV to ~1.0 eV. To verify our results we also calculated the same interface properties using the GGA functional. The most stable Pt/m-HfO<sub>2</sub> interfaces obtained with the LDA functional were re-optimized using GGA.

The comparison between LDA and GGA values for the Pt/m-HfO<sub>2</sub> interface properties considered here is shown in Table I and are within 0.2 eV from each other. From the VBO the Pt  $WF_{eff}$  on m-HfO<sub>2</sub> can be estimated from the relation:

$$WF_{eff} = BG_d + EA_d - VBO \quad (1)$$

where  $BG_d$  and  $EA_d$  are the dielectric's band gap and electron affinity, respectively. To roughly correlate interface stoichiometry with the calculated VBO's we used experimental values for  $BG_d$  and  $EA_d$  (5.7 eV [52] and 2.9 eV [53]) and the VBO's from Table I scaled by the experimental (5.7 eV) to calculated (3.9 eV) dielectric band gap ratio [54]. With this procedure we find that for stoichiometric interface conditions (0.5 ML-O) the Pt  $WF_{eff}$  is 5.7 eV and for O-poor interface conditions (0 ML-O) the Pt  $WF_{eff}$  is 4.4 eV. These numbers are in good agreement with work function data from a clean Pt(111) surface and with  $WF_{eff}$  for Pt on m-HfO<sub>2</sub>, respectively [17]. The comparison between the stoichiometric interface and the clean Pt surface is loosely justified by the assumption that those oxygen ions belong to the HfO<sub>2</sub> surface, not to the Pt surface. On the other hand, the good agreement between experimental and calculated  $WF_{eff}$ 's using the O-free interface is a strong indication that indeed the Pt/HfO<sub>2</sub> interface is highly reduced. Support to this conclusion comes from detailed studies of energy minimization of the Pt/m-HfO<sub>2</sub> interface in the presence of a silicon substrate [48]. This result offers a clear explanation to the large difference measured for the Pt vacuum and effective work functions [17].

**Table I.** Calculated valence band offset (VBO) using LDA and GGA exchange-correlation functionals for Pt/HfO<sub>2</sub> interfaces with different oxygen content.

	VBO(LDA), eV	VBO(GGA), eV
0ML	2.7	2.9
0.25ML	2.2	2.0
0.5ML	2.0	2.0
0.75ML	1.3	1.3
1ML	1.0	1.0

## B. Stoichiometry of the Mo/ZrO<sub>2</sub> interface

To investigate the impact of oxygen on the Mo WF in the presence of an interface with zirconia the atomic structures of the interfaces displayed in Figure 2 were fully optimized. The calculated PDOS for bulk zirconia together with the Fermi level positions for the stoichiometric and O-rich (0.5 ML of additional O atoms) Mo(110)/m-ZrO<sub>2</sub>(001) interfaces are shown in Figure 4.

The increase of oxygen concentration at the interface results in an upward energy shift of the zirconia valence band maximum (VBM) and consequently in a decrease of the Fermi level, decreasing the VBO by about 0.35 eV to ~2.40 eV from its value of ~2.75 eV for the stoichiometric case. Assuming as before  $BG_d = 5.7$  eV and  $EA_d = 2.9$  eV we obtain (after scaling the VBO)  $WF_{eff} = 4.25$  eV for the stoichiometric Mo/m-ZrO<sub>2</sub> case and 4.8 eV for the O-rich case, the latter in excellent agreement with the data of Yeo *et al.* [4].

Similar PDOS analyses were carried out for the reduced Mo/m-ZrO<sub>2</sub> (with less 0.5 ML O atoms with respect to the stoichiometric case – Figure 2d) and MoO<sub>x</sub>/m-ZrO<sub>2</sub> (1.5 ML additional O with sub-surface oxidation – Figure 2c) interfaces. The results of these calculations are summarized in Table II. The reduction of the Mo/ZrO<sub>2</sub> interface causes an opposite change of VBO (+0.4 eV without scaling) with respect to the stoichiometric interface. The changes of Mo  $WF_{eff}$  as a function of interface chemistry shown in Table II (the corresponding change in valence band offset is shown in Figure 4) are significantly smaller

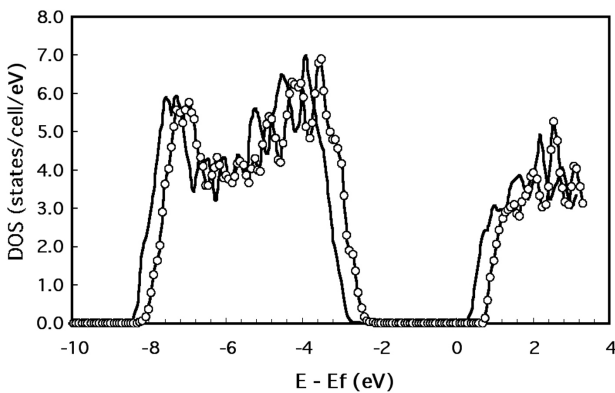


**Figure 4.** Density of states projected on the bulk part of the m-ZrO<sub>2</sub> slab for the stoichiometric (solid) and with extra 0.5 ML interfacial O (line with circles) Mo(110)/m-ZrO<sub>2</sub>(001) interfaces (from Ref. 49).

**Table II.** Mo(110)/m-ZrO<sub>2</sub> valence band offset for different interface stoichiometries.

Mo(110)/ZrO <sub>2</sub> with less 0.5 ML O	Mo(110)/ZrO <sub>2</sub> stoichiometric	Mo(110)/ZrO <sub>2</sub> with extra 0.5 ML O	Mo(110)/ZrO <sub>2</sub> with extra 1.5 ML O
+0.4 eV	0 eV	-0.35 eV	+0.2 eV

**Table III.** Charge distributions in the metal and oxide slabs with different Mo/m-ZrO<sub>2</sub> interface stoichiometries.

System	Mo(110)/ O-atom	Mo(110)/ ZrO <sub>2</sub>	Mo(110)+ 0.5 ML O/	Mo(110)+ 1.5 ML O/ ZrO <sub>2</sub>	ZrO <sub>2</sub> /O- atom ZrO <sub>2</sub>
Total metal charge	+0.52 e	+0.05 e	+0.55 e	+0.68 e	—
Total O-surface charge	-0.52 e	—	-0.70 e	-0.72 e	-0.28 e
Total Mo-atom charge	—	—	—	+1.21 e	—
Total O-sub-surface charge	—	—	—	-1.35 e	—
Total oxide charge	—	-0.05 e	+0.15 e	+0.17 e	+0.28 e

than the calculated changes of vacuum WFs (~2 eV for full surface oxidation and ~2.5 eV for surface and sub-surface oxidation [49]).

Table III shows that for the stoichiometric interface there is a negligible charge transfer from the metal slab to the oxide, while for the O-rich interface (0.5 ML extra O) it is significantly larger and is comparable to the calculated charge transfer in the Mo(110)/0.5 ML O-atom surface system. It also shows that there is less charge transfer from m-ZrO<sub>2</sub> to the additional interface oxygen atoms. We compared the oxide-interface dipole with the dipole formed between the oxide and the surface O-atom by calculating the charge transfer in the m-ZrO<sub>2</sub>(001)/0.5 ML O-adatoms system. As in the Mo surface case, the surface and interface charge transfers between the oxide and the O layer are similar. Therefore the charge transfers from the oxide and the metal to the interfacial O layer are comparable with their surface values and are opposite in direction, resulting in a partial dipole cancellation.

## C. Stability and Stoichiometry of WC/HfO<sub>2</sub> interface

The relative stabilities of the various interfaces with respect to the fully oxidized interface (4 O atoms per surface unit cell) are presented in Table IV. It is

**Table IV.** Calculated valence band offsets and thermodynamic stability of WC(0001)/m-HfO<sub>2</sub>(001) interfaces.

Interface	Relative stability, eV/surface unit cell	VBO (WM), eV	VBO (PDOS), eV
O full	0	2.6	2.5
C full	30.3	2.3	2.3
O half-filled	11.2	3.0	3.1
C half-filled	25.4	2.5	—
Empty (W-Hf)	24.5	3.2	—

seen that reduction of the fully oxidized interface by solid carbon is strongly endothermic. The same is valid for oxygen desorption from the interface: the energy required to remove one O<sub>2</sub> molecule from the fully oxidized interface to the gas phase is 11.2 eV. Notice that this value is significantly larger than the SiO<sub>2</sub> formation energy (about 9 eV), thus indicating that a fully oxidized HfO<sub>2</sub>/WC interface should be stable with respect to oxidation of the Si substrate. Additionally, in Table IV we present the calculated VBO's for all of the investigated interfaces. The calculated VBO for a full C ML at the interface (2.3 eV) is smaller than the value obtained for the model slab with a full O ML at the interface (2.6 eV). The WC  $W_{\text{eff}}$  on hafnia can be estimated using Eq. [1]. Here we employ  $BG_d = 5.65$  eV [55] and  $EA_d = 2.9$  eV [53], yielding  $W_{\text{eff}} = 5.95$  (6.25) eV for a full O (C) ML at the interface. These  $W_{\text{eff}}$  values are larger than experimental data which place the WC vacuum and effective (on HfO<sub>2</sub>) work functions in the range 4.5-5.0 eV [17].

For the WC/HfO<sub>2</sub> interface with a half O ML at the interface, the calculated VBO is 3.0-3.1 eV (see Table IV). This value is about 0.5 eV larger than the VBO for the interface with a full O ML. For the WC/HfO<sub>2</sub> interface with a half C ML at the interface, the calculated VBO is 0.3 eV higher than for the case of a full carbon ML. Similar to the band gap problem, calculated VBO values can be also underestimated as discussed previously for the Mo/ZrO<sub>2</sub> interface. If that happens then  $W_{\text{eff}}$  is overestimated as our results above indicate. To empirically correct the  $W_{\text{eff}}$  value we scaled the VBO by the experimental/theoretical band gap ratio. Proceeding in this way we obtain  $W_{\text{eff}} = 4.58$  (5.04) eV for a full O (C) ML at the interface, results that are more in line with the experimental data. This dependence of the VBO on the stoichiometry of the interface is similar to what we found previously for the Mo/ZrO<sub>2</sub> case and result from the smaller interface dipoles obtained for the O/C half-filled interfaces.

For the WC/HfO<sub>2</sub> interface with direct metal-metal bonds the calculated VBO is 3.2 eV, which is significantly larger than those with full O- and C-intermediate layers at the interface (2.3 eV – 2.6 eV). The large value of the VBO for the this case is expected due to the relatively small amount of charge transfer across the interface compared to the cases of O- and C- intermediate layers at the interface. This is a consequence of the electronegativity difference between W and Hf atoms, which is a lot smaller than between O (C) and W atoms. A C ML at the WC/HfO<sub>2</sub> interface gives rise to a 0.3 eV larger  $W_{\text{eff}}$  than an O ML at the interface (see Table IV). This is unexpected since oxygen is more electronegative than carbon which should result in a larger interface dipole

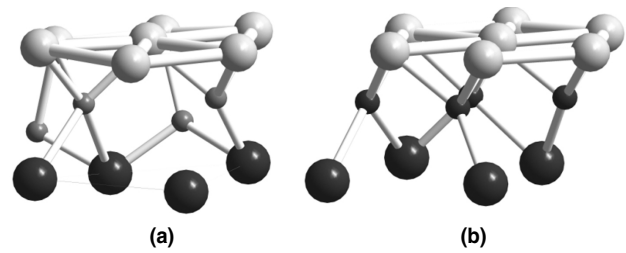


**Figure 5.** Optimized structures of the WC/HfO<sub>2</sub> interfaces with (a) one ML O and (b) one ML C interfacial layers. Large light gray: W; large dark gray: Hf; small medium gray: O; small dark gray: C (from Ref. 50).

in the case of oxygen, and therefore a larger  $W_{\text{eff}}$ . To understand the difference in VBO values for C- and O- interfacial MLs we calculated the vacuum WF of O-terminated WC(0001) (surface carbon layer replaced with O atoms). The resulting WF was 7.38 eV, which is about 0.9 eV larger than that for C-terminated WC(0001) (6.52 eV). Thus the calculated WC  $W_{\text{eff}}$ 's on HfO<sub>2</sub> cannot be directly correlated to its vacuum WF's. Instead, structural differences at the interface explain this behavior. As shown in Figure 4, while the relaxed interfacial oxygen ML has a structure similar to the topmost layer of m-HfO<sub>2</sub> (that is, it is split into two sub-layers with different heights from the tungsten layer), the relaxed interfacial carbon ML has a structure similar to the C-terminated WC slab (that is, all the interfacial C atoms are practically at the same height from tungsten layer).

In a separate calculation we found that swapping interfacial C with O in each of these two structures (WC-O/HfO<sub>2</sub> and WC-C/HfO<sub>2</sub>) results in higher energy configurations in both cases. This deceptively minor difference between the two structures significantly impacts the electrical properties. For example, the calculated VBO with an interfacial C-layer and a structure similar to the topmost oxygen layer of m-HfO<sub>2</sub> phase is 2.6 eV, which is higher than the value 2.3 eV obtained for the original (WC-like) structure, and is close to the VBO of the structure with an interfacial O-layer. Moreover, we made a direct integration of the electron density in the WC slab (between the two outermost W planes) on HfO<sub>2</sub> and found that the total number of electrons in the metal region for the case of interfacial C is smaller than for the case of interfacial O, indicating a larger charge transfer between the metal and the oxide for interfacial C, and confirming our VBO results.

#### D. GW correction to the band offsets

As previously explained, one can not compare VBO's obtained from DFT/LDA calculations to experimental values. Nevertheless the empirical procedure of scaling the VBO by the experimental to calcu-

lated dielectric band gap ratio provides some interesting conclusions. This technique has served as a motivation to look for a fully *ab-initio* procedure for calculating VBO's.

Within DFT applied for infinite systems the main source of error in the evaluation of the electronic levels and transition energies resides in the use of the Kohn-Sham eigenvalues. There is no theoretical justification for it, and in practice it is a well established fact that a Kohn-Sham DFT band structure calculation provides only semi-quantitative agreement with experiment, where the underestimation of the band gap for insulators is only one example. In fact, the only eigenvalue that makes sense in DFT is the last occupied level for a given finite system, which corresponds to the vertical ionization energy of the ground state [56]. Despite the development of modified and hybrid density functionals far more involved than the usual LDA the problem persists suggesting the need a more reliable and rigorous approach, that is to say, beyond DFT.

The GW approximation (GWA) to the many-body problem, as proposed by Hedin and Lundquist [57], offers this more accurate description of the band structure of materials, by treating explicitly the energy differences associated with the addition or the removal of one electron to/from the system. The method consists mainly in the evaluation of the self-energy  $\Sigma$  of the system, a unknown, non-local, energy-dependant and non-hermitian operator, which is approximated in GWA as the product of  $G$ , the Green function of the unperturbed system, and  $W = \epsilon^{-1}v$  the screened Coulomb potential. In this approach the equations to be solved assume the following form,

$$(T+V_{ext}+V_{harrree}) \psi_i^{qp}(r) + \int dr' \Sigma(r,r'; \epsilon_i^{qp}) \psi_i^{qp}(r') = \epsilon_i^{qp} \psi_i^{qp}(r) \quad (2)$$

where the eigenvalues  $\epsilon_i^{qp}$  are complex numbers, with their real parts equal to the energy of the pseudoparticles associated with the eigenfunctions  $\psi_i^{qp}$ . Note that this set of equations is formally equivalent to the Kohn-Sham equations if  $\Sigma(r,r'; \epsilon) = \delta(r-r') V_{xc}(r)$ . In practice, assuming that 1) the difference between  $\Sigma = GW$  and  $V_{xc}$  is small and 2) the Kohn-Sham wavefunctions are close to the pseudoparticle wavefunctions [58], one can use first order perturbation theory to correct the Kohn-Sham eigenvalues by evaluating

$$\epsilon_i^{qp} = \epsilon_i^{KS} + \langle \psi_i^{qp} | \Sigma(\epsilon_i^{qp}) - V_{xc} | \psi_i^{qp} \rangle \quad (3)$$

A difficulty arises when calculating  $\Sigma = GW$  because the  $W$  term involves the evaluation of the inverse dielectric function. This can be very time consuming, and usually it is approximated by a plasmon-pole model instead of a direct integration over

the energies [58,59]. Eventually, because GW is numerically demanding, calculations involving a hundred atoms or more are in general out of reach for today's computers. For this reason we here apply GW to calculate the bulk electronic structure of the oxides alone thus correcting the DFT band edges and DFT band offsets using the band edge shifts obtained with GW [59].

Using GWA as implemented in the Abinit code [60], we have calculated the VB and CB edge shifts for c-ZrO<sub>2</sub>, c-HfO<sub>2</sub>, and m-HfO<sub>2</sub>. The basis comprised of plane waves with a cut-off of 60 Ha for the Kohn-Sham states while the plasmon-pole model of Godby and Needs (as implanted in the Abinit code [60]) was employed to evaluate the  $W$  term. For Zr and Hf we have used the HGH pseudopotentials [61], including the semi-core levels 4s and 4p for Zr, and 5s and 5p for Hf (see [62] for the need of semi-core states in GWA calculations). We have reached an absolute numerical convergence of about 0.1 eV using 300 bands for the cubic phase of ZrO<sub>2</sub> and HfO<sub>2</sub>, and 700 bands for the monoclinic phase of HfO<sub>2</sub>. Different cut-offs for the inverse dielectric function and the self-energy have been chosen, between 20 and 35 Ha, with 8 K-points in the irreducible Brillouin zone. The results are summarized in Table V, with the ones of Králik *et al.* [63] also shown for comparison.

We obtained a good band gap for m-HfO<sub>2</sub> of 5.8 eV in comparison with experiments [52]. However we have noticed during the course of our calculations that it requires far more bands and higher cut-offs to achieve the same level of numerical convergence for the VBM and CBM shifts as for the band gap. Table V shows that our results for c-ZrO<sub>2</sub> do not compare well with the findings of Králik *et al.* [63]. Since our calculated band gap seems reasonable for m-HfO<sub>2</sub> we are quite as far as the general procedure of GW calculation is concerned. This discrepancy should be investigated further. It seems that there is still some room for convergence improvement by considering physics in the GW approach. More specifically, the inclusion of one more term in the self energy, the so-called  $\Gamma$  vertex contribution, could yield a correction larger than 0.1 eV.

In the previous sections we used an empirical scaling of the offsets to compare them or the related

**Table V.** Band gaps and band edge shifts in eV using GWA corrections for ZrO<sub>2</sub> and HfO<sub>2</sub>.

	DFT/LDA $E_{gap}$	GWA $E_{gap}$	VBM shift	CBM shift
c-ZrO <sub>2</sub> [63]	3.3 (X → $\Gamma$ )	5.6 (X → $\Gamma$ )	-1.2	1.0
c-ZrO <sub>2</sub>	3.2 (X → $\Gamma$ )	4.8 (X → $\Gamma$ )	-0.4	1.2
c-HfO <sub>2</sub>	3.8 (X → X)	5.6 (X → X)	-0.5	1.3
m-HfO <sub>2</sub>	4.0 ( $\Gamma$ → B)	5.8 ( $\Gamma$ → B)	-0.3	1.6

effective work function with experiment data. The scaling was given by the ratio between the experimental and the calculated (DFT) band gaps of the oxide. We now apply the band edge shifts obtained from GW calculations to correct our DFT band offsets in a more rigorous way. We use both our result and the result of Králik *et al.* [63] to correlate the calculated effective work functions to likely interface stoichiometries based on our interface models described before.

Using Králik's value of 1.2 eV [63] for the VBE shift, then our best match to the measured work function would be for an interface with some oxidation of TiN (VBO=3.9 eV), or some level (20%) of O vacancies at the interface (VBO=3.9 eV), or some amount of Ti-Hf bonding at the interface (for 100% Ti-Hf bonds at the interface the VBO=4.6 eV is out of the experimental range). So with this shift we can identify a few model interfaces for which the calculated VBO matches the experimental data. We can also eliminate some interface models based on a fully oxidized interface or for metal inter-mixing across the interface. Using our value of 0.3 eV for the shift the only model that comes close to the data is the fully reduced interface for which the calculated VBO is 3.7 eV. It is conceivable an interface of the type HfO<sub>2</sub>/HfO<sub>x</sub>/TiN with  $x < 2$  in which not only the interface is reduced but it is also sub-stoichiometric in the first MLs of HfO<sub>2</sub> away from the interface. In such a model the LDA VBO should increase a bit further and give us a better agreement with the data using the 0.3 eV shift. In fact, many HfO<sub>2</sub> samples show substoichiometric composition near the surface.

Let us now consider the Mo/ZrO<sub>2</sub> interfaces. With the 1.2 eV shift of Ref. [63] the best match is for a stoichiometric or over-oxidized interface since the experimental VBO is in the range 3.6-4.0 eV. On the other hand, using the 0.3 eV shift the conclusion is quite the opposite: the best match is for a partially to fully reduced interface.

Finally, for the WC/HfO<sub>2</sub> interface the experimental offset is in the range 3.6-4.5 eV. Using the 1.2 eV shift all interface models considered give offsets that fall within the range of experimental data values, except for a C-rich interface. Using the 0.3 eV shift only the fully reduced interface model matches the data.

### 3. CONCLUSION

We used first-principles calculations to investigate properties of the Pt/HfO<sub>2</sub>, Mo/ZrO<sub>2</sub>, and WC/HfO<sub>2</sub> interfaces, considering a wide range of interfacial oxygen content. The valence band offset was calculated as a function of oxygen concentration at the interfaces and used to obtain the metal effective

work function. The appropriate interfaces were inferred from the agreement between measured and calculated effective work functions. The best agreement for the Pt/HfO<sub>2</sub> and Mo/ZrO<sub>2</sub> cases using the empirical method of scaling the offset by the ratio of experimental to calculated band gaps correspond to fully reduced and fully oxidized interfaces, respectively. These results follow the oxygen affinity trend of the two metals: Mo is easily oxidized while Pt is more inert with respect to reaction with oxygen. This finding suggests an explanation to the difference between measured vacuum and effective work functions for Pt on HfO<sub>2</sub> as caused by strong interface reduction and for Mo on ZrO<sub>2</sub> as caused by interface oxidation. Hence, we propose the following general picture of Fermi pinning on oxides: metals that have low affinity for oxygen result in reduced interfaces and strong Fermi pinning, while metals with high affinity for oxygen produce oxidized interfaces and weak Fermi pinning. In addition, reducing conditions during processing may also result in reduced interfaces and strong Fermi pinning. Finally, the presence of oxygen plus nitrogen at the interface may also induce weak Fermi pinning as these two species have many similarities as far as binding to metals is concerned. This model offers a simple methodology for selecting metals that display weak Fermi pinning through the knowledge of their oxygen affinity.

Calculations of the band offsets using GW corrections to the band edges of the oxides lead to very different conclusions about the interface stoichiometry depending on the model used for GWA computations. Calculations by Králik *et al.* [63] yield a valence band edge shift for cubic ZrO<sub>2</sub> of 1.2 eV, while our calculations using the Abinit code [60] yield 0.3 eV and 0.5 eV for monoclinic and cubic HfO<sub>2</sub>, respectively. Applying these shifts to the band offsets calculated with DFT and for the interface models considered in this work we obtain very different conclusions: while applying the shift of Ref. [63] results in fully oxidized to partially reduced interfaces depending on the metal type, the use of our smaller shift indicates strongly reduced interfaces for all metal/oxide interfaces considered. More work is ongoing to clarify this matter further.

### ACKNOWLEDGEMENTS

We thank A. Knizhnik, A. Safonov, A. Gavrikov, and A. Bagatur'yants at Kinetic Technologies, J. Schaeffer, M. Stoker, and B. White at Freescale Semiconductor, Inc, and G. M. Rignanese at U. of Louvain-la-Neuve, for the fruitful discussions and the many suggestions provided during the course of this work.

## REFERENCES

- [1] The International Technology Roadmap for Semiconductors. <http://public.itrs.org>.
- [2] G. D. Wilk, R. M. Wallace, and J. M. Anthony, *J. Appl. Phys.* 87, 484 (2000).
- [3] C. C. Hobbs, L. R. C. Fonseca, A. Knizhnik, V. Dhandapani, S. B. Samavedam, W. J. Taylor, J. M. Grant, LuRae G. Dip, D. H. Triyoso, R. I. Hegde, D. C. Gilmer, R. Garcia, D. Roan, L. L. Lovejoy, R. S. Rai, E. A. Hebert, H.-H. Tseng, S. G. H. Anderson, B. E. White, and P. J. Tobin., *IEEE Trans. Elec. Dev.* 51, 971/978 (Part 1/Part 2) (2004).
- [4] Y. -C. Yeo, T. -J. King, and C. Hu, *J. Appl. Phys.* 92, 7266 (2002).
- [5] J. Robertson, *J. Vac. Sci. Technol. B* 18, 1785 (2000).
- [6] J. Bardeen, *Phys. Rev.* 71, 717 (1947).
- [7] V. Heine, *Phys. Rev.* 138, A1689 (1965).
- [8] S. G. Louie and M. L. Cohen, *Phys. Rev. B* 13, 2461 (1976).
- [9] S. G. Louie, J. R. Chelikovsky, and M. L. Cohen, *Phys. Rev. B* 15, 2154 (1977).
- [10] H. Hasegawa, and H. Ohno, *J. Vac. Sci. Technol. B* 4, 1130 (1986). [11] R. T. Tung, *Phys. Rev. Lett.* 52, 461 (1984).
- [12] D. R. Heslinga, H. H. Weitering, D. P. van der Werf, T. M. Klapwijk, and T. Himba, *Phys. Rev. Lett.* 64, 1589 (1990).
- [13] L. R. C. Fonseca and A. A. Knizhnik, *Phys. Rev. B* 74, 195304 (2006).
- [14] H. Michaelson, *J. Appl. Phys.* 48, 4729 (1977).
- [15] S. Samavedam, L. B. La, P. J. Tobin, B. E. White, C. C. Hobbs, L. R. C. Fonseca, A. A. Demkov, J. Schaeffer, E. Luckowski, A. Martinez, M. Raymond, D. H. Triyoso, D. Roan, V. Dhandapani, R. Garcia, S. G. H. Anderson, K. Moore, H.-H. Tseng, and C. Capasso, 2003 IEEE International Electron Devices Meeting 1, 13 (2003).
- [16] H. Y. Yu, M.-F. Lee, and D.-L. Kwong, *IEEE Trans. Elec. Dev.* 51, 609 (2004).
- [17] J. K. Schaeffer, L. R. C. Fonseca, S. B. Samavedam, Y. Liang, P. J. Tobin, and B. E. White, *Appl. Phys. Lett.* 85, 1826 (2004).
- [18] E. Cartier, F. R. McFeely, V. Narayanan, P. Jamison, B. P. Linder, M. Copel, V. K. Paruchuri, V. S. Basker, R. Haight, D. Lim, R. Carruthers, T. Shaw, M. Steen, J. Sleight, J. Rubino, H. Deligianni, S. Guha, R. Jammy, and G. Shahidi, *Symp. on VLSI Technology*, 230 (2005).
- [19] F. Fillot, B. Chenevier, S. Maitrejean, M. Audier, P. Chaudouet, B. Bochu, J. P. Senateur, A. Pisch, T. Mourier, H. Monchoix, B. Guillaumot, and G. Passemand, *Microelectronic Engineering* 70, 384 (2003).
- [20] S. J. Wang, H. Y. Tsai, and S. C. Sun, *Thin Solid Films* 394, 180 (2001).
- [21] Y. -M. Sun, S. Y. Lee, A. M. Lemonds, E. R. Engbrecht, S. Veldman, J. Lozano, J. M. White, J. G. Ekerdt, I. Emesh, and K. Pfeifer, *Thin Solid Films* 397, 109 (2001).
- [22] H. Romanus, V. Cimalla, J. A. Schaefer, L. Spieb, G. Ecke, and J. Pezoldt, *Thin Solid Films* 359, 146 (2000).
- [23] H. Hogberg, P. Tagtstrom, J. Lu, and U. Jansson, *Thin Solid Films* 272, 116 (1996).
- [24] K. L. Hakansson, H. I. P. Johansson, and L. I. Johansson, *Phys. Rev. B* 49, 2035 (1994).
- [25] J. Brillo, A. Hammoudeh, H. Kuhlbeck, N. Panagiotides, S. Schwegmann, H. Over, and H. -J. Freund, *J. Electron Spectroscopy and Related Phenomena* 96, 53 (1998).
- [26] M. Gothelid and E. Janin, *J. Phys.: Condens. Matter* 11, 773 (1999).
- [27] D. J. Siegel, L. G. Hector Jr., and J. B. Adams, *Surf. Sci.* 498, 321 (2002).
- [28] L. F. Mattheiss and D. R. Hamann, *Phys. Rev. B* 30, 1731 (1984).
- [29] J. Brillo, H. Kuhlbeck, and H. -J. Freund, *Surf. Sci.* 409, 199 (1998).
- [30] S. B. Zhang, M. L. Cohen, S. G. Louie, D. Tománek, and M. S. Hybertsen, *Phys. Rev. B* 41, 10058 (1990).
- [31] P. Hohenberg and W. Kohn, *Phys. Rev.* 136, B864 (1964); W. Kohn and L. J. Sham, *Phys. Rev.* 140, A1133 (1965).
- [32] G. Kresse and J. Furthmuller, *Phys. Rev. B* 54, 11169 (1996).
- [33] D. M. Ceperley and B. J. Alder, *Phys. Rev. Lett.* 45, 566 (1980); J. P. Perdew and A. Zunger, *Phys. Rev. B* 23, 5048 (1981).
- [34] J. P. Perdew and Y. Wang, *Phys. Rev. B* 45, 13244 (1992).
- [35] G. Kresse and J. Hafner, *J. Phys.: Condens. Mat.* 6, 8245 (1994).
- [36] <http://www.webelements.com>.
- [37] R. Ruh and P. W. R. Corfield, *J. Am. Ceramic Soc.* 53, 126 (1970).
- [38] A. Eichler, F. Mittendorfer, and J. Hafner, *Phys. Rev. B* 62, 4744 (2000).
- [39] H. Tang, A. Van der Ven, and B. L. Trout, *Phys. Rev. B* 70, 45420 (2004).
- [40] A. Eichler and J. Hafner, *Phys. Rev. Lett.* 79, 4481 (1997).
- [41] J. M. Soler, E. Artacho, J. D. Gale, A. Garcia, J. Junquera, P. Ordejon, and D. Sanchez-Portal, *J. Phys.: Condens. Matter* 14, 2745 (2002).
- [42] W. C. Topp and J. J. Hopfield, *Phys. Rev. B* 7, 1295 (1973).
- [43] N. Troullier and J. L. Martins, *Phys. Rev. B* 43, 1993 (1991).
- [44] G. Kresse, J. Hafner, *J. Phys.: Condens. Mat.* 6, 8245 (1994).
- [45] J. W. Edwards, R. Speiser, H. L. Johnston, *J. Appl. Phys.* 22, 424 (1951).
- [46] C. J. Howard, E. H. Kisi, R. B. Roberts, R. J. Hill, *J. Am. Ceramic Soc.* 73, 2828 (1990).
- [47] R. C. Weast, *CRC Handbook of Chemistry and Physics*, 67th ed., CRC Press, Boca Raton, FL, 1983.
- [48] A. V. Gavrikov, A. A. Knizhnik, A. A. Bagatur'yants, B. V. Potapkin, L. R. C. Fonseca, M. W. Stoker, and J. Schaeffer, *J. Appl. Phys.* 101, 14310 (2007).
- [49] A. A. Knizhnik, I. N. Iskandarova, A. A. Bagatur'yants, B. V. Potapkin, and L. R. C. Fonseca, *J. Appl. Phys.* 97, 64911 (2005).
- [50] A. A. Knizhnik, A. A. Safonov, I. N. Iskandarova, A. A. Bagatur'yants, B. V. Potapkin, L. R. C. Fonseca, and M. W. Stoker, *J. Appl. Phys.* 99, 84104 (2006).
- [51] C. G. Van de Walle and Richard M. Martin, *Phys. Rev. B* 34, 5621 (1986).
- [52] S. Sayan, E. Garfunkel, and S. Suzer, *Appl. Phys. Lett.* 80, 2135 (2002).
- [53] T. E. Cook, Jr., C. C. Fulton, W. J. Mecouch, R. F. Davis, G. Lucovsky, and R. J. Nemanich, *J. Appl. Phys.* 94, 7155 (2003).
- [54] This procedure is justified by the band gap underestimation in DFT, which is likely to affect the calculated valence band offset.
- [55] R. Puthenkovilakam and J. P. Chang, *Appl. Phys. Lett.* 84, 1353 (2004).
- [56] R. M. Martin, *Electronic Structure: Basic Theory and Practical Methods* p. 144, Cambridge University press (2004).
- [57] L. Hedin and S. Lundquist, *Solid State Physics*, 23 (1969) p.1.
- [58] M.S. Hybertsen and S. G. Louie, *Phys. Rev. B* 34, 5390 (1986).
- [59] S. Lebègue, B. Arnaud, M. Alouani and P.E. Bloechl, *Phys. Rev. B* 67, 155208 (2003).
- [60] X. Gonze, G.-M. Rignanese, M. Verstraete, J.-M. Beuken, Y. Pouillon, R. Caracas, F. Jollet, M. Torrent, G. Zerah, M. Mikami, Ph. Ghosez, M. Veithen, J.-Y. Raty, V. Olevano, F. Bruneval, L. Reining, R. Godby, G. Onida, D.R. Hamann, and D.C. Allan. *Zeit. Kristallogr.* 220, 558-562 (2005).
- [61] C. Hartwigsen, S. Goedecker and J. Hutter, *Phys. Rev. B* 58, 3641 (1998).
- [62] M. Rohlfing, P. Krüger and J. Pollmann, *Phys. Rev. Lett.* 75, 3489 (1995).
- [63] B. Králic, E. K. Chang, and S. G. Louie, *Phys. Rev. B* 57, 7027 (1998).